Zeolites as Pheromone Dispensers

J. Muñoz-Pallares, A. Corma, J. Primo, and E. Primo-Yufera*

Instituto de Tecnología Química, UPV-CSIC, Universidad Politécnica de Valencia,
Avenida de los Naranjos s/n, 46022 Valencia, Spain

Modification of the chemical and structural properties of zeolites has led to the preparation of an optimized zeolitic dispenser for insect attractants such as *n*-decanol and trimedlure. The impact of zeolite variables such as the framework Si/Al ratio, nature of compensating cation, nature and strength of acid groups, and pore dimensions on the kinetics of emission has been studied, and the results are as follows. Zeolite pore dimensions and the presence or absence of acid sites have the greatest effect on the rate of release, decreasing with decreasing pore diameter and increasing acidity. Further tuning of the release characteristics is achieved by controlling the polarity and the polarizability of the framework by increasing the Si/Al ratio and nature of the compensating cations, i.e., the higher the polarizability and the lower the polarity, the slower the release of attractants.

Keywords: *Pheromone; dispenser; controlled release; emission kinetics; zeolites*

INTRODUCTION

The use of semiochemicals against harmful insects has important ecological advantages such as high specificity, biodegradability, and low toxicity. The main applications for their use as specific attractants are monitoring, mass and lethal trapping, and sexual confusion. In all cases, dispensers with controlled rates of emission of the attractants are required for a longer life.

Effective dispensers must meet four basic requirements. (1) The kinetic emission must be close to zero-order and close to the optimum velocity which depends on the field conditions, the intensity of the pest, and the type of treatment being employed (monitoring, trap and kill, or mating disruption) to decrease the level of pheromone consumption and the number of applications required. (2) The dispenser must be adaptable to emission requirements, i.e., pheromone employed, type of treatment, and climate conditions. (3) The emission of volatile pheromone mixtures must be accurate and proportional. The majority of insect pheromones are complex mixtures of compounds, which often have different volatilities, and they must be emitted in adequate proportions during the treatment (*1*). (4) The dispensers should respect the environment.

The commercially available dispensers most commonly used are three-layered foils with different permeabilities and sizes, microcapsules made from various polymers, or polymeric tubes, cylinders, or disks containing the pheromone (*2–5*).

Looking for better semiochemical dispensers, we have investigated the zeolites. These aluminosilicates have a network of channels and cavities with pore diameters in the range of 0.7–1.2 nm. They have been used successfully as catalysts (*6*), for ion exchange purposes (*7*), and consequently in the formulation of detergents,

and as carriers for insecticides and fragrances (*8*). An important characteristic of the zeolites is their high adsorption capacity and the possibility of adapting their characteristics to optimize the host−guest interactions (*6*). Thus, by selection of zeolite composition and pore diameter, it is possible to control the rate of diffusion of molecules in and out of the micropores, and consequently, it should be possible to achieve controlled and prolonged release of adsorbed semiochemicals.

In addition, the simultaneous use of two or more zeolites with different adsorption and diffusion properties should allow for the correct emission of complex mixtures of substances with various polarities and volatilities. Another important advantage of zeolitic dispensers is that they are environmentally friendly, as they are incorporated into the soil as a clay.

For nonpolar molecules, like the majority of pheromones, the predominant determinants of adsorption are medium-range or van der Waals forces. The intensity of adsorption depends on the size of the adsorbed molecule and the polarizability of the zeolitic network. However, in some cases, hydrogen bonds and other heteropolar interactions may occur.

The objective of this study is to develop a better understanding of zeolitic materials with respect to their interactions with semiochemicals in an effort to design more effective and more adaptable dispensers. Thus, we show the influence of the geometric and chemical parameters of zeolites with respect to their adsorption capacity, emission, and diffusion rate for *n*-decanol (sexual pheromone from *Agrotis segetum*) and trimedlure.

MATERIALS AND METHODS

Materials. Zeolites differing in their Si/Al ratio, polarity, compensating cation, Brönsted acidity, and pore size were used for this study.

(a) Faujasites. The crystal structure forms three-dimensional pores with diameters of 0.74 nm. The junction of four pores forms a wide cavity (known as a supercage) with a diameter of 1.2 nm, and smaller cavities (sodalite box) with internal diameters of 0.5 nm. Between the sodalite boxes are

---

* To whom correspondence should be addressed: Instituto de Tecnología Química, UPV-CSIC, Universidad Politécnica de Valencia, Avda. de los Naranjos s/n, 46022 Valencia, Spain. Telephone: 34(96)3877800. Fax: 34(96)3877809. E-mail: eprimo@itq.upv.es.

4802 *J. Agric. Food Chem.,* Vol. 49, No. 10, 2001

Muñoz-Pallares et al.

hexagonal channels with an internal diameter of 0.22 nm. These channels are too small to allow the access of pheromone. The compensating cations tend to accumulate inside the zeolitic network, occupying the most energetically favorable positions. The faujasite-type samples used in this work are as follows.

(1) Commercial Faujasites. XNa (Sigma Aldrich Química S. A., Madrid, Spain): 1.3 Si/Al ratio; unit cell of $[Al_{28}Si_{109}O_{384}]$-$Na_{83}\cdot240H_2O$.

YNa (CBV1OO, P. Q. Zeolites B. V., AH Drachten, The Netherlands): 2.6 Si/Al ratio; unit cell of $[Al_{53}Si_{139}O_{384}]Na_{53}\cdot240H_2O$.

(2) Faujasite Samples Prepared in House. USYNa: 5.7 Si/Al ratio; unit cell of $[Al_{28}Si_{164}O_{384}]Na_{28}\cdot240H_2O$. XNaCs: 1.3 Si/Al ratio; unit cell of $[Al_{83}Si_{109}O_{384}]Na_{42}Cs_{41}\cdot240H_2O$. YHNa 10%: 2.6 Si/Al ratio; unit cell of $[Al_{53}Si_{139}O_{384}]$-$H_{5.3}Na_{47.7}\cdot240H_2O$. YHNa 50%: 2.6 Si/Al ratio; unit cell of $[Al_{53}Si_{139}O_{384}]H_{27}Na_{26}\cdot240H_2O$. YHNa 80%: 2.6 Si/Al ratio; unit cell of $[Al_{53}Si_{139}O_{384}]H_{43}Na_{10}\cdot240H_2O$.

(b) Zeolite ZSM-5. This zeolite has a system of interconnected pores formed by rings of 10 tetrahedrons. There are two types of pores, which at the intersections form junctions with a diameter of ~0.9 nm. Straight pores have an elliptic cross section with its half-axis measuring 0.53 nm × 0.56 nm, and zigzag pores also have an elliptic cross section with its half-axis measuring 0.51 nm × 0.54 nm.

The following ZSM-5 zeolite samples were prepared for this study. ZSM-5 Na 20: 20 Si/Al ratio; unit cell of $[Al_{4.5}Si_{91.5}O_{192}]$-$Na_{4.5}\cdot16H_2O$. ZSM-5 Na 400: 400 Si/Al ratio; unit cell of $[Al_{0.25}Si_{95.75}O_{192}]Na_{0.25}$.

(c) Beta Zeolite. This zeolite is characterized by a tridimensional systems of pores which are formed by 12 member rings. On the *a* and *b* axes, the pores are straight and have the same pore diameter (0.76 nm × 0.64 nm). On the *c* axis, they have a smaller pore diameter (0.5 nm × 0.5 nm) and are slightly curved. The junction of three pores forms a cavity that measures between 0.9 and 1 nm in diameter.

The following Beta zeolites were prepared for this study. Beta Na 30: 30 Si/Al ratio; unit cell of $[Al_2Si_{62}O_{128}]Na_2$. Beta Na 400: 400 Si/Al ratio; unit cell of $[Al_{0.16}Si_{63.4}O_{128}]Na_{0.16}$.

Adsorbates. The adsorbates used in this study are *n*-decanol, which is the female sexual pheromone from *A. segetum* and *Cydia pomonella*, and trimedlure, the male synthetic attractant for *Ceratitis capitata* [*tert*-butyl 4(5)-chloro-2-methylcyclohexane carboxylate]. The structural features of *n*-decanol are common to many types of pheromones and are characterized by a large nonpolar chain and a relatively polar group at one end.

In the case of trimedlure, the functional polarity is low and its capacity to form hydrogen bonds is reduced by both the ester function and the interference of the tertiary butyl group.

Methods for the Preparation and Modification of the Noncommercial Zeolites. *(a) USYNa.* The USYNa was prepared by exchanging 80% of the Na⁺ content in the original NaY with NH₄⁺. The sample was calcined at 600 °C for 3 h in steam. During this treatment, the zeolite was partially dealuminated, resulting in a framework Si/Al ratio of 5.8.

(b) XNaCs 50%. The zeolite XNa was subjected to ionic exchange using a 1 M CsCl solution, then washed, and dried at 110 °C. Chemical analysis indicated a 32% exchange. The process was repeated until a 50% exchange was achieved.

(c) Zeolite Y with Different Percentages of Sodium Exchanged for Hydrogen. The starting material, commercially available YNa, was subjected to an exchange treatment with NH₄NO₃ (0.15 M). The mixture was incubated at 80 °C for 6 h with stirring, filtered and washed to eliminate sodium ions, and then dried at 110 °C. The preparation was calcined as follows: the temperature was increased from 25 to 350 °C over the course of 150 min, maintained at 350 °C for 120 min, increased to 500 °C over the course of 150 min, and maintained at this temperature for 180 min. This protocol produced a 10% exchange, as determined by chemical analysis. The X-ray diffraction indicated a crystallinity of 93% compared to that of the commercially available YNa. The same procedure, but starting with NH₄NO₃ (0.5 M), was used to obtain YHNa 50%.

To obtain YHNa 80%, YHNa 50% was subjected two times to the exchange procedure with NH₄NO₃ (0.5 M) and calcined as described above. The percent exchange was confirmed by chemical analysis, and the results of the X-ray diffraction indicated a crystallinity of 81% compared to that of the commercially available YNa.

(d) ZSM-5 Na. The initial gel was formed with silica, Na₂O, tetrapropylammonium hydroxide, aluminum hydroxide, and water. After being stirred, the sample was crystallized at 140 °C in Teflon-lined stainless steal autoclaves for 7 days. It was washed by centrifugation, dried at 130 °C, and calcined (heating until 530 °C over the course pf 360 min and maintaining at this temperature for 720 min). The different Si/Al ratios are obtained by modifying the proportion of silica and aluminum hydroxide in the initial gel.

(e) Beta Na. The initial gel was formed with NaCl, KCl, and tetraethylammonium hydroxide in water, and silica is added while stirring. After 30 min, a solution of sodium aluminate is added and the mixture is stirred for an additional 30 min. The final gel is crystallized at 135 °C in rotating Teflon-lined stainless steal autoclaves over the course of 24 h. The sample is centrifuged, washed with distilled water till pH 9, and dried at 100 °C. Finally, it is calcined at 580 °C for 3 h. The different Si/Al ratios are obtained by modifying the ratio between the amounts of silica and aluminum hydroxide in the initial gel.

Techniques Used for the Characterization of the Zeolites. Crystalline structures were verified by X-ray diffraction, by comparing the patterns of diffraction of the prepared zeolites with those of published standards (*9*). The crystallinity was determined by comparing the areas of the most intense peaks with those of a standard whose crystallinity is 100% (*10*). A Phillips PW 1830 apparatus, with an automatic aperture, and Kα radiation of Cu were used.

Aluminum content was determined by atomic absorption and the amount of alkaline metals by flame emission using a Varian Spectra 10 Plus instrument.

The analyses were performed with 50 mg of the solid sample calcined at 200 °C and treated with 1 mL of HF (48%) and 1 mL of HNO₃ (60%) at 40 °C. The samples were maintained in airtight polypropylene containers for 24 h, until the sample was completely dispersed. Distilled water (milli-Q) was then added to a final volume of 50 mL.

The number and strength of the acidic centers were determined by assessing the adsorption and desorption of pyridine by solid-state infrared spectroscopy (IR) (*11*) using an FTIR NICOLET 710 spectrophotometer. The samples were prepared as 10 mg/cm² self-supporting tablets, and they were incubated for 12 h at 400 °C, under a vacuum pressure of 1.33×10^{-2} Pa. The pyridine was adsorbed at room temperature and then allowed to desorb in a vacuum at different temperatures. The pyridine interacts with the central Brönsted acids forming the pyridinium ion, which produces a characteristic IR band (1545 cm⁻¹), and the intensity of the band is determined by the number of acidic centers. The intensity of this band, after desorption at varying temperatures, is used to estimate the number of centers of distinct acidic forces.

Study of the Relationship between the Characteristics of the Zeolites and Their Emission Kinetics. *(a) Preparation of Zeolitic Tablets.* The required amount of pheromone, dissolved in CH₂Cl₂, was added to the zeolite in powder form and homogenized to obtain the desired initial loading. After removal of the solvent, the initial load was confirmed by extraction and quantitative GLC using an internal standard.

The powders were molded into cylindrical tablets using a manual hydraulic press and working at 10.2 Tm/cm², except when studying the effect of pressure, where 3.1 Tm/cm² was also used. Unless specified, tablets with diameters of 5, 13, and 20 mm were used.

(b) Determination of Emission Kinetics. For each trial, 10 tablets were used. Two were kept for initial loading measurements, and eight were placed in an aerator, with an air flow rate of 80 mL/min at 25 °C. The values reported are the average of two determinations. The aerator is a glass cylinder
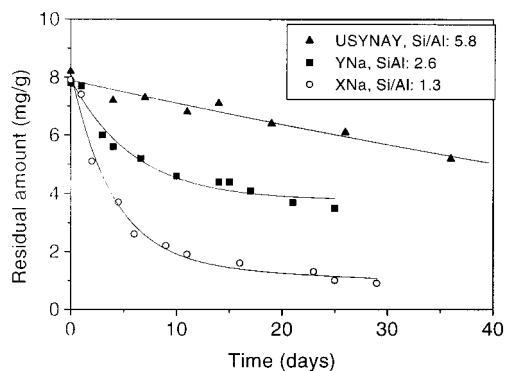
Zeolites as Pheromone Dispensers

J. Agric. Food Chem., Vol. 49, No. 10, 2001 **4803**

Figure 1. Emission of *n*-decanol adsorbed on faujasites with different Si/Al ratios. Experiments were carried out with an initial loading of 8 mg of 10 OH/g of zeolite, with 13 mm Ø tablets weighing 0.55 g. The compression force was 3.1 T/cm², with an aeration flow rate of 80 mL/min, at 25 °C.
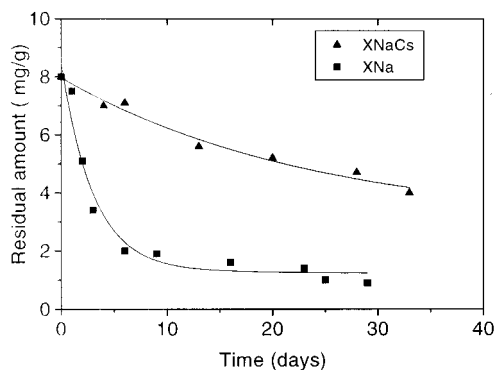

Figure 2. Emission of *n*-decanol adsorbed on X zeolites with varying compensating cations. The conditions are the same as those described in the legend of Figure 1.
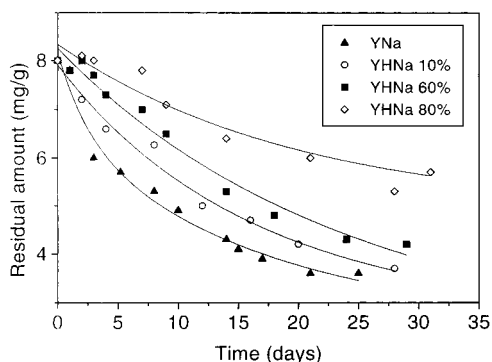

Figure 3. Emission of *n*-decanol adsorbed on NaY and NaHY zeolites with varying acidic forces. The conditions are the same as those described in the legend of Figure 1.

Figure 4. Emission of trimedlure adsorbed on Y zeolites with varying acidic strengths. The conditions are the same as those described in the legend of Figure 1.

Figure 5. Emission of *n*-decanol adsorbed on zeolites with varying pore sizes and low Si/Al ratios. Experiments were carried out with an initial loading of 140 mg of 10 OH/g of zeolite, with 5 mm Ø tablets weighing 70 mg. The compression force was 10.2 T/cm², with an aeration flow rate of 80 mL/min, at 25 °C.

Figure 6. Emission of *n*-decanol adsorbed on zeolites with varying pore sizes and high Si/Al ratios. The conditions are the same as those described in the legend of Figure 5.

which has a diameter of 12 cm and a height of 10 cm. There is a porous plate at the base of the cylinder whose pore size is 160 µm × 250 µm. It functions to uniformly distribute the air that enters through the lower pipe. Glass filters with porous plates can be used.

The air was maintained at a constant temperature by a heating strip, which is activated by a temperature controller. This controller consists of a Fuji PYW-4 digital temperature regulator, a thermopar, and manual output control. The tablets were placed on a grate and distributed in a circle, at the same distance from the wall of the cylinder, not touching one another, so that they were maintained at the same temperature.

Periodically, the tablets were extracted in Soxhlet, with ethanol or CH₂Cl₂, and the residual loading was determined by quantitative chromatography using an internal standard (2.3 mg of tetradecanol). Each sample was injected five times,
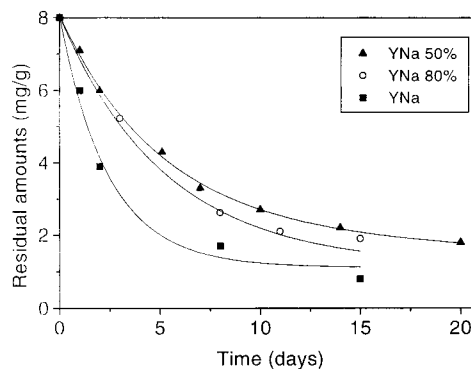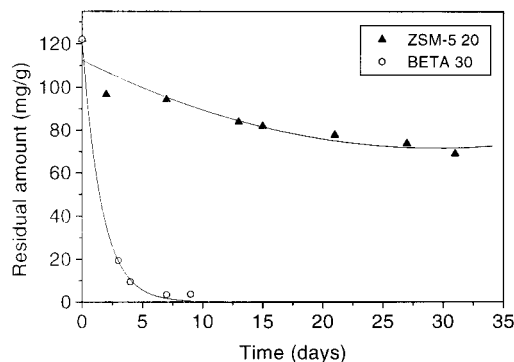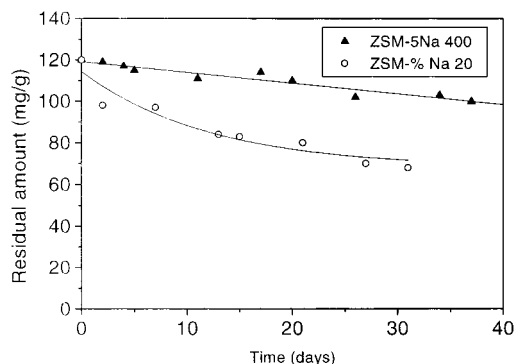
and the average values and standard errors for each data set were determined.

A Fisons GC8000 chromatograph was used with a flame ionization detector connected to a Fisons DP8000 integrator: Teknokroma-TR-Wax (polyethylene glycol) column (30 m × 0.25 nm); phase thickness, 0.25 µm; carrier gas, helium; flow rate, 30 mL/min; split ratio, 1/5; injection temperature, 250 °C; detection temperature, 250 °C; and temperature program, 3 min at 80 °C, from 80 to 180 °C over the course of 25 min, and 2 min at 180 °C.

The normal duration of these assays is 1 month, with eight extractions; four are taken during the first 10 days when the system is most rapidly emitting. The data are then plotted to depict the residual amount of semiochemical versus time (Figures 1−9). The results are fitted to a first-order kinetic rate equation, and the following kinetic parameters are
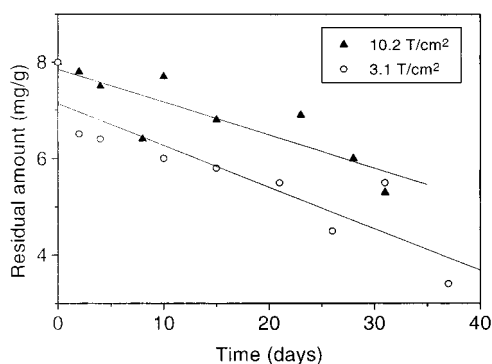
4804 *J. Agric. Food Chem.,* Vol. 49, No. 10, 2001

Muñoz-Pallares et al.

Figure 7. Emission of *n*-decanol adsorbed on YHNa 80%, compressed with different forces. Experiments were conducted with an initial loading of 8 mg of 10 OH/g of zeolite, with 5 mm Ø tablets weighing 70 mg and an aeration flow rate of 80 mL/min, at 25 °C.
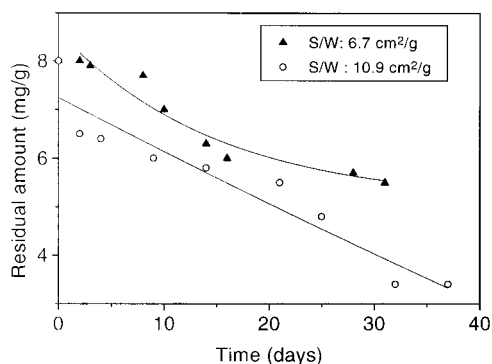

Figure 8. Emission of *n*-decanol adsorbed on the zeolite YHNa 80% with varying surface/weight ratios. Experiments were performed using an initial loading of 8 mg of 10 OH/g of zeolite, a compression force of 3.1 T/cm², and an aeration flow rate of 80 mL/min, at 25 °C.

Figure 9. Emission of *n*-decanol adsorbed on the zeolite XNa with varying surface/weight ratios. Experiments were performed using an initial loading of 8 mg of 10 OH/g of zeolite, a compression force of 3.1 T/cm², and an aeration flow rate of 80 mL/min, at 25 °C.
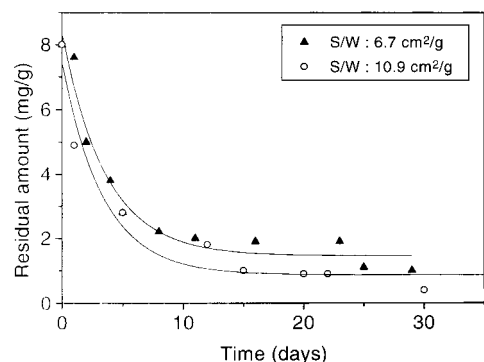
calculated: kinetic constant K, half-life [using $t_{1/2} = (\ln 2)/K$], and the correlation coefficient (r) with the adjusted exponential curve for first-order kinetics.

RESULTS AND DISCUSSION

Influence of the Si/Al Ratio on Emission Kinetics. *(a) Zeolites with Faujasite Structure.* We have compared the emission of *n*-decanol (10 OH) from three zeolites with the same faujasite structure (large pore, 0.74 nm) but containing distinct Si/Al ratios. The corresponding emission values (±SD) are given in Figure 1 and kinetic parameters in Table 2. The

Table 1. Polarities of the Faujasites That Were Used

zeolite	Si/Al ratio	no. of polarity sites/unit cell
USYNa	5.8	20
YNa	2.6	53
XNa	1.3	83

Table 2. Parameters Obtained after Adjusting the Experimental Data in Figure 1 to First-Order Kinetics

	XNa	YNa	USYNa
kinetic constant K (days^{-1})	0.065	0.031	0.011
correlation coefficient (r)	0.888	0.903	0.935
half-life ($t_{1/2}$) (days)	10 ± 1.3	22 ± 2.6	60 ± 5.6

Table 3. Polarities of the ZSM-5 Zeolites That Were Used

zeolite	Si/Al ratio	no. of polarity sites/unit cell
Na ZSM 5−20	20	4.5
Na ZSM 5−400	40	0.25

Table 4. Characteristics of the Zeolites That Were Used

zeolite	cationic radii (Å) (Pauling)	charge/radii ratio
XNa	0.95	0.43
XNaCs	1.69	0.27

Table 5. Parameters Obtained after Adjusting the Experimental Data Shown in Figure 2 to First-Order Kinetics

	XNa	XCs
kinetic constant K (days^{-1})	0.065	0.19
correlation coefficient (r)	0.888	0.977
half-life ($t_{1/2}$) (days)	10 ± 1.3	36 ± 2.2

experimental data are in good agreement with first-order kinetics, as reflected by the high correlation coefficients and low standard deviations of $t_{1/2}$. The initial loading used (8 mg of 10 OH/g of zeolite) ensures that saturation effects, which would interfere with the results, are not produced. In addition, the pore size of 0.74 nm allows for a highly mobile adsorbate.

The experimental data indicate that the emission velocity decreases when the Si/Al ratio increases. This indicates that a stronger adsorption of *n*-decanol occurs when the polarity of the oxygen bonds is lower and the polarizability of the network is higher, showing that by increasing the framework composition it is possible to approach a zero-order kinetics while increasing up to 6-fold the half-life of emission.

Structurally, the increase of the Si/Al ratio corresponds to a decrease in the number of compensating cations and also in the fraction of negative charge interacting in the oxygen (*12, 13*), producing an increase in the polarizability.

Since the van der Waals interactions are proportional to the polarizability of the zeolitic network, which increases with the increase in the Si/Al ratio, it can be concluded that the predominant intermolecular force (27.7 kcal/mol) corresponds to the van der Waals interactions which represent 67% of the alcohol−zeolite interaction, even in the case of the most polar zeolite, XNa (*14*).

(b) ZSM-5 Zeolites. To study the influence of pore diameter on the rate of diffusion of the semiochemical, a ZSM-5 zeolite which has smaller pores has been used as an adsorbent (Figures 5 and 6 and Table 9).

With ZSM-5 zeolite and regardless of the framework Si/Al ratio, the level of retention is much higher, and with an initial charge of 8 mg of 10 OH/g of ZSM-5, no significant losses were detected during 1 month of aeration.

Table 6. Parameters Obtained after Adjusting the Experimental Data Shown in Figure 3 to First-Order Kinetics

	YNa	YHNa 10%	YHNa 50%	YHNa 80%
kinetic constant K (days^{-1})	0.031	0.028	0.026	0.014
correlation coefficient (r)	0.903	0.968	0.971	0.935
half-life ($t_{1/2}$) (days)	22 ± 2.6	24.4 ± 1.7	26.5 ± 1.6	50 ± 4.7

Table 7. Parameters Obtained after Adjusting the Experimental Data in Figure 4 to First-Order Kinetics

	YNa	YHNa 50%	YHNa 80%
kinetic constant K (days^{-1})	0.145	0.077	0.098
correlation coefficient (r)	0.961	0.934	0.882
half-life ($t_{1/2}$) (days)	4.7 ± 0.3	9 ± 0.8	7 ± 1.5

Table 8. Polarities and Pore Dimensions of the Zeolites That Were Used

zeolite	pore dimensions (Å)	Si/Al ratio
Beta 30	7.6×5.4	30
ZSM-5 20	5.3×5.6	20
Beta 400	7.6×5.4	400
ZSM-5 400	5.3×5.6	400

Table 9. Parameters Obtained after Adjusting the Experimental Data in Figures 5 and 6 to First-Order Kinetics

	Beta 30	Beta 400	ZSM-5 20	ZSM-5 400
kinetic constant K (days^{-1})	0.397	0.042	0.015	0.005
correlation coefficient (r)	0.898	0.775	0.876	0.792
half-life ($t_{1/2}$) (days)	2 ± 0.3	16 ± 3.7	47 ± 6.8	136 ± 30

Influence of the Compensating Cation. To study the influence of the extraframework composition of the zeolite, Cs^+ was exchanged with Na^+, resulting in a faujasite X sample with an extraframework cation content of 50% Na^+ and 50% Cs^+ (XNaCs 50).

The *n*-decanol emission values and the respective parameters obtained with this sample are shown in Figure 2 and Table 5, where they are compared with those obtained with the NaX zeolite.

One can observe that the kinetics of emission are much slower when 50% of the cations are Cs^+ (lower charge/radius ratio). The exchange of Na^+ for Cs^+ creates an increase in polarizability due to the electronic structure of Cs^+ and an increase in the level of van der Waals interactions with the adsorbed molecule. Moreover, the preferred location of the Cs^+ in the cationic positions closest to the supercage favors the interaction and produces a higher level of adsorption of the semiochemical.

Influence of the Presence of Brönsted Acid Sites and Their Strength on Emission Kinetics. The emission kinetics of two zeolites, with different Brönsted acid concentrations and strengths, were tested with two pheromones, *n*-decanol and trimedlure.

(a) n-Decanol with Acidic Zeolites. Isostructural zeolites of the faujasite type with different H^+ concentrations (YNa, YHNa 10%, YHNa 50%, and YHNa 80%) were used. The emission kinetics and the kinetic parameters are shown in Figure 3 and Table 6. As expected, the highest levels of retention are observed with the most acidic zeolites. The presence of Brönsted acid centers introduces a decisive factor in the adsorp-tion strength of the functional groups which are able to form hydrogen bonds, and the level of interaction increases when the acidity of the zeolite increases. Indeed, Zicovich-Wilson (*15*) and Shah et al. (*16*), when studying the interaction between alcohols and acid sites, found that the hydrogen of the hydroxyl group weakly interacts with the oxygen adjacent to the aluminum (bond length, 0.162 nm) and that the hydrogen of the zeolite strongly interacts with the oxygen of the hydroxyl group of the alcohol (bond length, 0.142 nm), forming an electrically neutral, stable complex. Furthermore, it can be expected that Na^+-H^+ exchange on the zeolites that were tested has two effects: (a) increasing the proportion of hydrogen atoms by simple substitution of the sodium and (b) increasing the strength of the acid centers by alteration of the network composition. The treatment used to substitute the Na^+ for H^+ in the YNa zeolite produces, as a secondary effect, the removal of aluminum from the network during the calcination step that is necessary to decompose the NH_4^+ and to form the acid sites. This removal of aluminum is more pronounced when the level of exchange is higher. Given that the polarity of the Al$-$O bond is greater than that of the Si$-$O bond, the loss of Al from the network produces a decrease in the oxygen charge and more acidic O$-$H groups are then generated. Thus, the sample with the highest level of exchange and highest number of Brönsted acid centers, which has lost more Al, is more acidic, this also contributing to the higher observed level of retention. The acidity of the samples has been measured by programmed thermodesorption of pyridine, which shows that the only sample where a band characteristic of the pyridinium ion (1545 cm^{-1}) was observed in the IR spectrum after calcinations at 450 °C was the YHNa 80%.

(b) Trimedlure with Acidic Zeolites. We have also studied the emission kinetics of trimedlure adsorbed on three isostructural zeolites with varying Na^+-H^+ exchange percentages (YNa, YHNa 50%, and YHNa 80%), and the obtained emission values and the kinetic parameters are shown in Figure 4 and Table 7. The results indicate that when acidic groups are introduced in the zeolites, the level of retention of the trimedlure is increased by the interaction between the oxygens of the ester groups and the acidic groups. The level of retention, for a given acidity, is lower with trimedlure than with *n*-decanol. This observation may be attributed to the lower capacity of the ester group as opposed to the alcohol group to form hydrogen bonds, and also to the steric hindrance of the ester tertiary butyl group of the trimedlure. It should be noticed that with the most acidic YHNa 80% sample a partial hydrolysis of the ester group was observed which alters the kinetic results, and also decreases the effectiveness of the semiochemical.

Influence of the Size and Characteristics of the Pores on Emission Kinetics. The influence of zeolite pore diameter on the kinetics of desorption has been studied using two different zeolite structures (ZSM-5 and Beta) which have similar Si/Al ratios (Table 8). The values of emission and the kinetic parameters are shown in Figures 5 and 6 and Table 9. It can be seen there that the level of retention increases as the pore size decreases; ZSM-5 20, which has a smaller pore size, retains more *n*-decanol than Beta 30. When the pore diameter is smaller, the interaction of the adsorbate with the walls of the zeolites is stronger; this effect,

4806 *J. Agric. Food Chem.,* Vol. 49, No. 10, 2001

Muñoz-Pallares et al.

Table 10. Parameters Obtained after Adjusting the Experimental Data in Figure 7 to First-Order Kinetics

compression force	3.1	10.2
kinetic constant K (days^{-1})	0.020	0.011
correlation coefficient (r)	0.937	0.777
half-life ($t_{1/2}$) (days)	34 ± 3.2	65 ± 0.7

Table 11. Parameters Obtained after Adjusting the Experimental Data in Figures 8 and 9 to First-Order Kinetics

	YHNa 80%		XNa	
tablet diameter (mm)	13	5	13	5
surface/weight ratio (cm^2/g)	6.7	10.9	6.7	10.9
kinetic constant K (days^{-1})	0.014	0.020	0.065	0.083
correlation coefficient (r)	0.934	0.937	0.888	0.937
half-life ($t_{1/2}$) (days)	50 ± 4.7	34 ± 4.7	10 ± 1	8.3 ± 0.7

together with the geometrical constraints, decreases the rates of desorption and emission.

Also, the slightly polar zeolite, ZSM-5, which has the smallest pore size, has the slowest desorption kinetics. Comparison of the kinetics of Beta 30 with those of Beta 400 and comparison of the kinetics of ZSM-5 20 with those of ZSM-400 demonstrate that the retention of the less polar zeolites is stronger. These results confirm the influence of the pore size and also the results obtained with the faujasites on the influence of the framework Si/Al ratio. The initial load of 140 mg of 10 OH/g of zeolite ensures that the internal volume is not saturated.

Modification of the Kinetics by Changes in Tablet Preparation. *(a) Influence of the Compression Force.* We compared YHNa 80% tablets that had two different compression forces: 3.1 and 10.2 T/cm^2. The emission values and kinetic parameters are shown in Figure 7 and Table 10.

The level of retention was observed to increase when the compression force increases. Thus, Figure 7 shows that the kinetics with 10.2 T/cm^2 are closer to zero-order and the half-life is almost double than in the case when 3.1 T/cm^2 was applied. A higher compression force decreases the size of the macropores of the tablets, decreasing the diffusion rate of the adsorbed molecules.

The compression force is the easiest parameter to vary, and it has an important effect on the emission kinetics; nevertheless, it has some limitations. For instance, in some samples, with large initial loadings it is not possible to increase the compression force above a certain limit since the tablet will exude part of the adsorbed substance. On the other hand, for certain zeolites, excessive pressure could alter the crystal structure and result in undesired changes in the chemical properties.

(b) Influence of the Surface/Weight Ratio. The influence of the surface/weight ratio was tested for two zeolites (YHNa 80% and XNa) with tablets with 6.7 and 10.9 cm^2/g, with *n*-decanol as the adsorbate. The emission values and the kinetic parameters are shown in Figures 8 and 9 and Table 11.

In all cases, the emission rate was observed to increase as the surface/weight ratio increases. A surface/weight ratio increase of 61%, in the case of YHNa 80%, decreases that half-life by 32%, while in the case of XNa, the same increase in the surface/weight ratio caused a 17% decrease in the half-life.

CONCLUSIONS

The emission kinetics of the different zeolites indicate that these microporous materials are suitable as semiochemical dispensers.

For any given pheromone and application, it is possible to increase or decrease the level of retention by varying the Si/Al ratio, the size of the compensating cation, the Brönsted acid strength (for pheromones that can form hydrogen bonds), and the pore diameter and by modifying the compression pressure and the surface/weight ratio of the tablets.

With these modifications, emission kinetics could approach zero-order, avoiding large initial emissions velocities, which result in significant losses of pheromone.

Via application of these same criteria, it should be possible to develop dispensers containing a combination of zeolites that can accommodate mixtures of two or more pheromone components maintaining the proportional emission similar to the natural one.

To use zeolites as pheromone dispersers, it is necessary to consider the possibility that they may be altered by catalytic active sites in the zeolitic network.

LITERATURE CITED

(1) Knight, A. L.; Howell, J. F.; McDonough, L. M.; Weiss, M. Mating Disruption of Codling Moth (Lepidoptera: Tortricidae) with Polyethylene Tube Dispensers: Determining Emissions Rates and the Distribution of Fruit Injuries. *J. Agric. Entomol.* **1995**, *12*, 85−99.

(2) Hendricks, D. E. Polyvinyl Chloride Capsules: a New Substrate for Dispensing Tobacco Budworm (Lepidoptera: Noctuidae) Sex Pheromone Baits Formulations. *Environ. Entomol.* **1982**, *11*, 1005−1010.

(3) Kehat, M.; Dunkelblum, E.; Gothilf, S. Mating Disruption of the Cotton Leafworm, *Spodoptera littoralis* (Lepidoptera: Noctuidae), by Release of Sex Pheromone from Widely Separated Hercom-Laminated Dispensers. *Environ. Entomol.* **1983**, *12*, 1265−1269.

(4) Bradley, S. J.; Suckling, D. M.; McNaughton, K. G.; Wearing, C. H.; Karg, G. A Temperature-Dependent Model for Predicting Release Rates of Pheromone from a Polyethylene Tubing Dispenser. *J. Chem. Ecol.* **1995**, *21* (6), 745−760.

(5) Cork, A.; Basu, S. K. Control of the Yellow Stem Borer, *Scirpophaga incertulas,* by Mating Disruption with a PVC Resin Formulation of the Sex Pheromone of *Chilo suppresalis* (Lepidoptera: Pyralidae) in India. *Bull. Entomol. Res.* **1996**, *86*, 1−9.

(6) Corma, A. Inorganic Solids Acids and Their Use in Acid-Catalysed Hydrocarbon Reactions. *Chem. Rev.* **1995**, *95*, 559−614.

(7) Breck, D. W. *Zeolite Molecular Sieves: Structure, Chemistry and Use*; John Wiley: London, 1974; pp 427−433.

(8) Colgate Palmolive Co. Perfume-Containing Carrier Having Surface-Modified Particles for Laundry Composition. U.S. Patent 4,536,315, 1985.

(9) von Ballmoos, R. *Collection of Simulated XRD Powder Patterns for Zeolites*; Butterworths Scientific Limited, Guilford, U.K., 1984.

(10) ASTM. *Standards for Catalysis. D-3942-80*; ASTM: West Conshohocken, PA, 1985.

Zeolites as Pheromone Dispensers

J. Agric. Food Chem., Vol. 49, No. 10, 2001 **4807**

(11) Corma, A.; Fornés, V.; Forni, L.; Marquez, F.; Martínez-Triguero, J.; Moscotti, D. 2,6-Di-*tert*-Butyl-Pyridine as a Probe Molecule to Measure External Acidity of Zeolites. *J. Catal.* **1998**, *179*, 451−458.

(12) Barthomeuf, D. Catalysis and Adsorption by Zeolites. Acidity and Basicity in Zeolites. *Stud. Surf. Sci. Catal.* **1991**, *65*, 157−169.

(13) Dwyer, J. Evaluation and Tailoring of Acid−Base Properties of Zeolites, Part 2. *Zeolites Microporous Solids: Synth., Struct. React.* **1992**, 321−345.

(14) Kiselev, A. V. *Molecular Sieve Zeolites*; Advances in Chemistry Series; American Chemical Society: Washington, DC, 1971; Vol. 102, pp 37−45.

(15) Zicovich-Wilson, C. M.; Viruela, P.; Corma, A. Formation of Surface Methoxy Groups on H-Zeolites from Methanol. A Quantum Chemical Study. *J. Phys. Chem.* **1995**, *99*, 13221−13231.

(16) Shah, R.; Gale, J. D.; Payne, M. C. Methanol Adsorption in Zeolites: A First Principles Study. *J. Phys. Chem.* **1996**, *100*, 11688−11697.